Foreword

The polymer and plastics industries have had a profound techno-economic impact on society for almost a century. In fact, it has been suggested that the advent and use of polymers and plastics products have represented a revolutionary technological change. They are used in packaging, furniture, construction materials, automotive, aerospace, sporting goods, biomedical, electronics, communications, and so on. More importantly, they have adapted to the ever changing social and technological demands. Thus, many of the current popular products, such as smart phones, computers, and other technological innovations would be difficult to contemplate in the absence of polymers. It does not seem likely that the foreseeable future will see a reduction in the important role that polymers and plastics will play in future technological development.

Cognizant of the role that polymers played and will continue to play in our lives, a group of polymer scientists and engineers from various countries around the world founded the Polymer Processing Society (PPS) in March 1985 at the University of Akron, Akron, Ohio, USA. According to its constitution, the goal of the PPS is to foster scientific understanding and technical innovation in polymer processing by providing a discussion forum in the field for the worldwide community of engineers and scientists. Thus, PPS has attempted to achieve this goal using the following mechanisms:

1. Organization of annual and regional conferences rotating among the various regions of the world and the dissemination of technical content of the conferences in the form of proceedings.
2. The publication of the International Polymer Processing (IPP) Journal.
3. The publication of the Progress in Polymer Processing (PPP) Series.

So far, these activities have allowed the PPS and its members to exchange information and ideas about the evolution of the principles and methods of polymer science and engineering and their application to the generation of innovative products, processes and applications.

Since the formation of PPS, eleven PPP volumes have been published. Four distinguished leaders in the polymer processing field have served as series editors: Leszek Utracki, Warren Baker, Kun Sup Hyun, and James L. White. Last summer at PPS 29 in Nuremberg, Germany, I was asked by the Executive Committee of PPS to serve as

PPP series editor. It is my hope, that with the help of the Advisory Editorial Board, our colleagues in the polymer processing field, and Hanser Publications, to publish at the rate of about one book every year. We already have two books under preparation. I encourage prospective authors to contact me or any of the Advisory Board members with their ideas and suggestions.

One of my first tasks has been to follow and expedite the completion of Film Processing Advances. This has given me the opportunity to refresh and expand my contacts with the editors, Drs. Kanai and Campbell, whom I have known for many years. As I have done some work in the area of film processing, I always benefited from reading their works and meeting them at conferences. Thus, it was easy to work together with them and with the publisher, Hanser, to set up the necessary mechanisms and procedures for a smooth and timely finish for this ambitious project. It is a real pleasure to have Film Processing Advances as the first PPP project completed during my first term as a series editor. Obviously, the credit goes to Professors Campbell and Kanai and to the contributors of the chapters for their tireless efforts. We also owe special thanks to the editorial staff at Hanser, especially Ms. Cheryl Hamilton, who handled the details of publication smoothly and efficiently.

As we all know, plastic films represent a major component of the polymer and plastics business. Plastic films are used extensively in packaging products. They have withstood and adapted to various pressures and requirements. Film processing technology continues to advance with the advent of improved extrusion and die design technologies, development of advanced film blowing and casting techniques; temperature, orientation, and crystallization control, and advanced computer simulation, monitoring and control systems. Thus, the publication of Film Processing Advances, by the same editors of the successful Film Processing, represents a timely technical update on the status of film processing technology.

Finally, on behalf of the Polymer Processing Society and the PPP Editorial Advisory Board, I would like to express our sincerest thanks and appreciation for Professor Gregory Campbell and Professor Toshitaka Kanai for the immense amount of effort, time, and dedication that they have contributed to the editing and preparation of this book. I also wish to thank the other authors for contributing their excellent chapters. Also, we owe a lot of thanks to Ms. Cheryl Hamilton and other Hanser staff for the organization of the copyediting of the book and timely completion of this project.

Musa R. Kamal
Series Editor

1 Extruder and Screw Design for Film Processing

Mark A. Spalding and Gregory A. Campbell

1.1 The Extrusion Process 2
1.2 Rate Calculation 9
1.3 Gels 12
1.4 Troubleshooting Extrusion Processes 17
1.4.1 Improper Shutdown of Processing Equipment 18
1.4.2 Gel Showers in a Cast Film Process 19
1.4.3 Unmixed Gels 21
1.4.4 Carbon Specks in a Film Product 22
1.4.5 Rate Limitation Due to a Worn Screw 23

Single-screw extruders are the preferred machines for plasticating and metering resin to downstream film processes. The extruder must provide a homogenous and stable extrudate at high rates and at the target discharge temperature and pressure. Moreover, gels must be at a low and acceptable level. Gels are defined as any particle that creates an optical defect in the film. Because film products are typically very thin and in the range of 15 to 250 μm, very small particles can cause observable defects. In many cases, these particles are created in the extruder, and thus screw design can be used to mitigate gels from the final film product.

This chapter will describe the single-screw extrusion process typically used for film processes, common screw designs, troubleshooting operations, and common gel defects that originate from the extruder. In-depth operation and fundamentals of the process are beyond the scope of this writing. The reader can learn more about the fundamentals of single-screw extrusion and troubleshooting in reference 1.

1.1 The Extrusion Process

All single-screw extruders have several common characteristics. The main sections of the extruder include the barrel, a screw that fits inside the barrel, a motor drive system for rotating the screw, and a control system for the barrel heaters and motor speed. A schematic for an extruder is shown in Fig. 1.1. Many innovations on construction of these components have been developed by machine suppliers over the years. A hopper is attached to the barrel at the entrance end of the screw, and the resin is typically fed by gravity (flood fed) into the feed section of the screw. The resin is typically purchased in pellet form (most polyolefins for example), but powders are common (PVDC resin). Recycle film from edge trim is often chopped and metered into the hopper. The extruder screw must first convey the pellets away from the feed opening, melt the resin, and then pump and pressurize it for a downstream filming process. This type of machine is referred to as a plasticating, single-screw extruder. The barrel is usually heated with a minimum of three temperature zones. These different temperature zones are consistent with the three functions of the screw: solids conveying, melting, and pumping or metering of the resin.

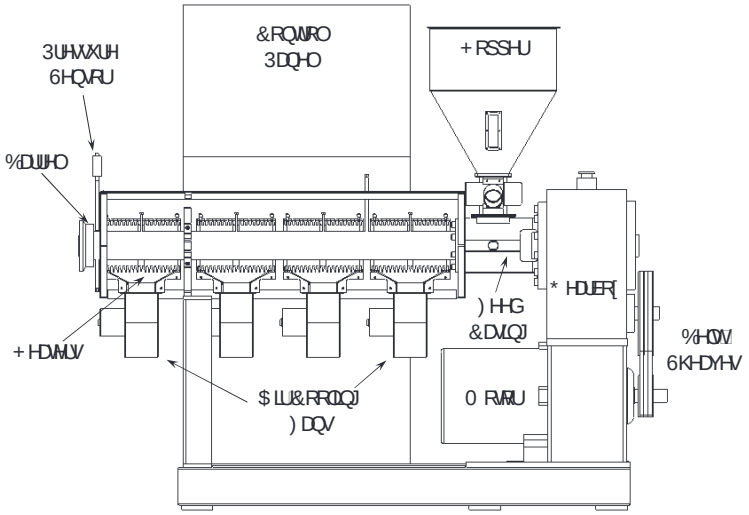

Figure 1.1 Schematic of a typical plasticating, single-screw extruder with a smooth-bore feed section. The extruder is equipped with four barrel heating and cooling zones and a combination belt sheave gearbox speed reduction drivetrain (courtesy of William Kramer of American Kuhne)

The single-screw plasticating process starts with the mixing of the feedstock materials. Typically, several different feedstocks are added to the hopper such as fresh resin pellets, recycle material, additives, and a color concentrate. Often these components need to be blended prior to adding them to the hopper. Next, the feedstock flows via gravity from the hopper through the feed throat of the feed casing and into the solids conveying section of the screw. Typically this feed casing is cooled using water. The feed section of the screw is typically designed with a constant depth and is about 4 to 8 barrel diameters in axial length. Directly after the solids conveying section is a section where the channel depth tapers to a shallow-depth metering section. The tapered depth section is commonly referred to as the transition or melting section. In general, the metering section is also a constant depth, but many variations exist where the channels oscillate in depth. The metering section pumps and pressurizes the material for the downstream unit operations including static mixers, screen filtering devices, and dies. The total length of the extruder screw and barrel is typically measured in barrel diameters or as a length-to-diameter (L/D) ratio. Section lengths are often specified in barrel diameters or simply diameters.

A conventional single-flighted screw is shown in Fig. 1.2. This screw has a single helix wound around the screw root or core. Multiple-flighted screws with two or more helixes started on the core are very common on high-performance screws. Screws with barrier flighted melting sections are very common in film processes because they provide high rates with lower discharge temperatures. Barrier melting sections have a secondary barrier flight that is located a fraction of a turn downstream from the primary flight, creating two flow channels in the transition section:

a solids melting channel and a melt conveying channel. Barrier flighted sections will be discussed in more detail later. Many high-performance screws [1] have two or more flights in the metering section of the screw. The screw is rotated by the shank using either specially designed splines or by keys with rectangular cross sections. The mathematical zero position of the screw is set at the pocket where the screw helix starts. Most extruder manufacturers rotate the screw in a counterclockwise direction for viewers positioned on the shank and looking towards the tip. This rotation convention, however, is not standard.

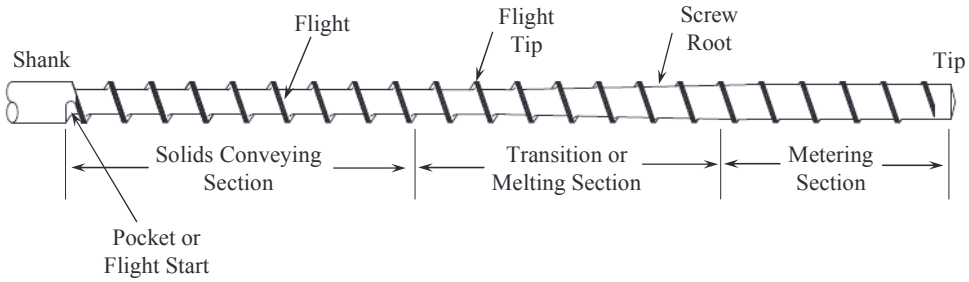

Figure 1.2 Schematic of a typical single-flighted screw (courtesy of Jeff A. Myers of Robert Barr, Inc.)

The flight is a helical structure that is machined into the screw and extends from the flight tip to the screw core or root. The flight has a width at the flight tip called the flight land. The small clearance between the flight land and the barrel wall minimizes the flow of resin over the land. The polymer that does flow between the clearances supports the screw and centers it in the barrel. The radial distance between the flight tip and the screw root is referred to as the local flight height or channel depth. The feed section usually has the largest channel depth and provides the largest cross-sectional volume in the screw. The deep channel conveys the relatively low bulk density feedstock pellets into the machine via the motion of the helix. The feedstock is conveyed forward into the transition section or melting section of the screw. The transition section increases in root diameter in the downstream direction, and thus the channel depth is decreasing. Here, the feedstock is subjected to higher pressures and temperatures, causing the feedstock to compact and melt. As the material compacts, its bulk density can increase by a factor of nearly two or more. As the feedstock compacts, the entrained air between the pellets is forced backwards and out through the hopper. For example, a pellet feedstock such as low density polyethylene (LDPE) resin can have a bulk density at ambient conditions of 0.58 g/cm^3, while as a fully compacted solid bed in the transition section the density will approach 0.92 g/cm^3 before melting starts. Thus for every unit volume of resin that enters the extruder, about 0.4 unit volumes of air must be expelled through the voids in the solid bed and then discharged through the hopper. The transition section is where most of the polymer is converted from a solid to a fluid. The fluid is then conveyed to the metering section where the molten resin is pumped to the

discharge opening of the extruder. In general, the metering section of a conventional screw has a constant root diameter, and it has a much smaller channel depth than the feed section. The ratio of the channel depth in the feed section to the channel depth in the metering section is often referred to as the compression ratio of the screw.

The transition section shown in Fig. 1.2 is a conventional single-flighted design. These designs are still used for film operations, but barrier flighted melting sections are much more common. Barrier flighted melting sections will typically provide higher rates, lower discharge temperatures, a more stable discharge pressure, and extrudates that have fewer gels due to poor mixing. Barrier flighted melting sections are constructed by positioning a second flight (or barrier flight) in the transition section such that the solids are maintained on the trailing side and the molten resin on the pushing side. A schematic of a barrier flighted screw with an Egan (or spiral Maddock-style) mixer is shown by Fig. 1.3. A schematic of a cross section of a barrier melting section is shown in Fig. 1.4. The resin that is melted near the barrel wall is conveyed across the barrier flight and collected in the melt conveying channel. The key design parameters include the position of the barrier flight, the depths of the channels, and the undercut clearance on the barrier flight. The undercut clearance is measured by positioning a segment of straight bar stock across the two main flights and then measuring the gap between the bar and the barrier flight land. For most designs, the barrier flight undercut is constant for the entire length of the section. As a very general rule, the undercut is typically about 0.01 times the diameter of the screw. Undercuts that are smaller than this rule, however, are often used. The position of the barrier flight sets the width of both channels. Many styles of barrier melting screws are commercially available, and many different variations of the channel widths and depths are used commercially.

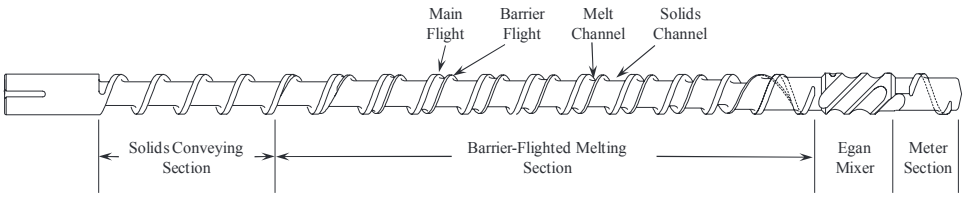

Figure 1.3 Schematic of a Steward barrier flighted screw with a downstream dispersive (Egan) mixer (courtesy of William Kramer of American Kuhne)

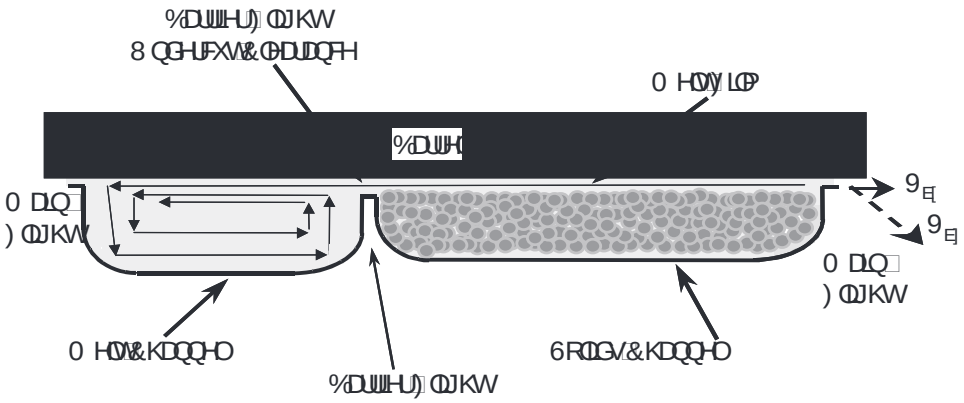

Figure 1.4 Cross-sectional view of a barrier melting section

Solid polymer fragments often exit the solids channel of barrier sections, or they can be discharged from conventional melting sections, especially at high rates and screw speeds. These solids need to be trapped and dispersed before the extrudate is shaped into film. Maddock-style mixers are typical dispersive mixers that are used for this application, but other mixers or high-performance sections are used. An Egan mixer (spiral Maddock-style mixer) is shown in Fig. 1.3 while other Maddock mixer styles are shown in Fig. 1.5.

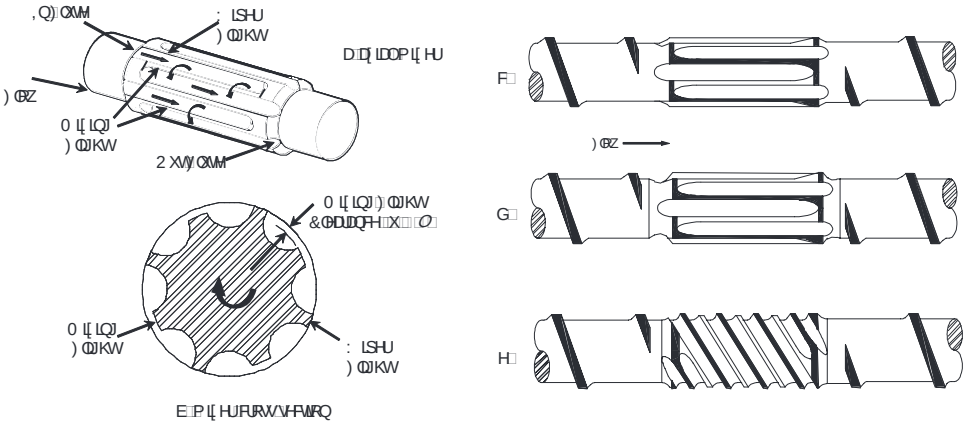

Figure 1.5 Schematic for Maddock-style mixers. (a) A mixer with the flutes aligned in the axial direction; (b) a cross-sectional view perpendicular to the screw axis showing the clearance for the mixing flight; (c) a mixer with the flutes aligned in the axial direction; (d) an axial mixer with pressure relief zones at the entry and exits; (e) an Egan mixer with spiral flutes (courtesy of Jeff A. Myers of Robert Barr, Inc.)

Maddock-style mixers [2] are very commonly used due to their low cost to manufacture and their ability to disperse solid fragments, trap and melt polymer solids, and mitigate color and compositional gradients. Many styles are on the market under two basic types: (1) flutes parallel to the screw axis, and (2) flutes in a spiral pattern

in the same direction as the flights. Schematics for these devices are shown by Fig. 1.5. For small-diameter screws, the mixer is generally constructed with four inflow flutes (or channels) and four outflow flutes. Larger diameter screws will have more paired flutes due to the larger available area at the screw circumference. For a Maddock mixer with the flutes parallel to the axis of the screw, molten polymer flows into the inflow flutes via a pressure gradient and then either continues to flow downstream in the flute or is passed through a small clearance between the mixing flight and the barrel wall. This small clearance is responsible for providing the dispersive mixing characteristics of the device. Screw manufacturers typical specify the mixer flight height position relative to the main flight as an undercut. The undercut u for a 63.5 mm diameter screw is typically about 0.5 to 1.2 mm, although for some applications and designs the clearance can be smaller. For this size screw with an undercut of 0.50 mm and a flight clearance of 0.07 mm, the clearance between the mixing flight and the barrel wall is 0.57 mm. The material that flowed across the mixing flight is accumulated in the outflow flute and is then flowed via pressure to the discharge end of the mixer. The wiper flight shown in Fig. 1.5 is set at the same height as the flight in the metering section. For mixers with the flutes in a spiral pattern, some of the forwarding flow in the flutes is due to the rotational movement of the flute relative to the barrel wall. Performance and simulation details can be found in the references [3, 4].

The specification of the undercut on the mixing flight for Maddock-style mixers is critical to its performance. As previously stated, all material must flow through the clearance provided by the sum of the undercut and flight clearance. If the clearance is too large, some medium- and small-size solid polymer fragments will not be trapped and melted by the device. If the clearance is too small, then a high-pressure gradient can occur, and there exists the possibility of increasing the temperature of the resin beyond its thermal capabilities, that is, causing degradation. The shear stress that the material experiences for flow across the mixing flight of the mixer can be estimated using Eqs. 1.1 and 1.2. The shear stress level is responsible for breaking up agglomerates and dispersing solid polymer fragments. A higher shear stress level will improve the ability of the mixer to disperse smaller size fragments. This shear stress calculation is based on screw rotation physics and is as follows:

$$\dot{\gamma}_M = \frac{\pi(D_b - 2u - 2\lambda)N}{(u + \lambda)} \tag{1.1}$$

$$\tau_M = \eta\dot{\gamma}_M \tag{1.2}$$

where $\dot{\gamma}_M$ is the average shear rate for flow over the mixing flight in 1/s, u is the undercut clearance on the mixing flight, λ is the mechanical clearance of the flights, N is the screw rotation rate in revolutions/s, η is the shear viscosity at the temperature of the mixing process and at shear rate $\dot{\gamma}_M$, and τ_M is the shear stress that the

material will experience for flow over the mixing flight. The stress level for flow across the mixing flight is typically between 50 and 200 kPa.

Several other design factors are important for the correct operation of Maddock-style mixers. These include the positioning of the mixer downstream from the melting section, the distance between where the meter flight ends and the mixer starts, and the elimination of resin stagnation regions. The mixer must be positioned on the screw downstream far enough such that only low levels of solid polymer fragments exist. If the level of solids is too high in the stream, then the fragments may be melted and dispersed at a rate slower than the rate of the entering solids, causing the mixer to become plugged with solids and reducing the rate of the machine. As shown in Fig. 1.5, the mixer should be positioned about 0.3 to 0.5 diameters away from the end of the upstream metering section flight. This creates an annular gap where the material is allowed to flow evenly into all inflow flutes of the mixer. The annular gap is often undercut as shown by Fig. 1.5(d). If the flights extend close to the mixer entry, then it is possible that the inflow flute near the trailing side of the flight will not operate completely full of resin and thus may cause the resin to stagnate and degrade. Moreover, flute depths should be streamlined and shallower at the entry end of the outflow flute and the exit end of the inflow flute. A common design error is to make these regions too deep, creating stagnation regions and causing resin degradation.

As an example of process design, linear low density polyethylene (LLDPE) resin is commonly used for blown film, cast film, and extrusion coating processes. Even though the resin grades are similar (melt indices or MIs do vary) for these three processes, the extrusion equipment is significantly different due to the requirements of the die and downstream equipment. The blown film process requires an extrudate that is relatively low in temperature and typically in the range of 200 to 220°C. In order to plasticate and produce an extrudate in this temperature range the metering channel is relatively deep and the screw would be designed to rotate at speeds less than 100 rpm. For a 150 mm diameter screw with a square-pitch lead length ($L = D_b$), the metering channel depth (H) would be between 9 and 12 mm. The cast film process requires an extrudate that is slightly higher in temperature and typically in the range of 240 to 260°C. The same 150 mm diameter screw would have a metering channel depth of 6 to 9 mm and the screw would rotate at higher speeds. The extrusion coating process requires an extrudate that is very high in temperature and often approaching 310°C. Here the metering channel depth would typically be about 3 to 4 mm for the 150 mm diameter screw, and the screw would be designed to rotate at very high speeds up to 230 rpm. These examples clearly show that the extrudate temperatures are set in part by the geometry of the metering section channel, the conditions of the process, and the MI of the resin.

The specific rate is often a good measure of the relative discharge temperature for a process. The specific rate is simply the rate divided by screw speed. For the exam-

ples above, the specific rate for the metering channels would be the highest for the blown film screw with the deep metering channel and the lowest for the extrusion coating process screw with the very shallow channel. Thus as a general guideline, the extrudate temperature decreases when the specific rate of the screw increases at constant barrel diameter. The specific rates for the screws in these examples increased because the channel depth increased. The specific rate could also be changed by adjusting the lead length. The calculated specific rotation rate can be also used as a similar guideline for discharge temperature. This guideline, however, can be violated if the channel is extremely deep and a large positive pressure gradient exists [1].

1.2 Rate Calculation

For smooth-bore extruders, the rate of the extruder is controlled by the metering section of the screw. The expected rate for the process can be calculated based on the geometry of the metering channel, screw speed, pressure gradient, and the melt density and shear viscosity for the resin. The basic screw geometry for a single-flighted (p = 1) metering channel is shown in Fig. 1.6.

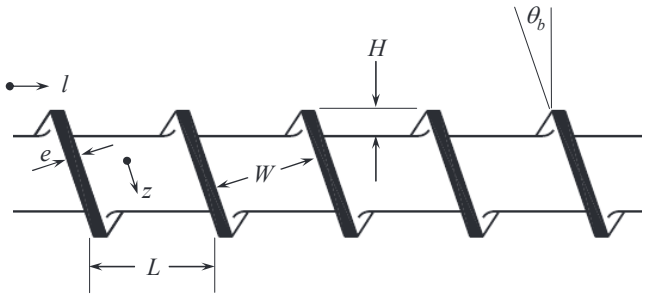

Figure 1.6 Geometric parameters for a single-flighted screw in the wound state

Two driving forces for flow exist in the metering section of the screw. The first flow is due just to the rotation of the screw and is referred to as the rotational flow component. The second component of flow is due to pressure gradients that exist in the z direction, and it is referred to as pressure flow. The sum of the two flows must be equal to the overall flow rate. The overall flow rate, Q, the rotational flow, Q_d, and the pressure flow, Q_p, for a constant depth metering channel are related as shown in Eq. 1.3. The subscript d is maintained in the nomenclature for historical consistency even though the term is for screw rotational flow rather than the historical drag flow concept. The method described here was developed by Rowell and Finlayson [5, 6] and later modified by Tadmor and Klein [7].

$$Q = Q_d - Q_p \tag{1.3}$$

The volumetric rotational flow term (Q_d) depends on the several geometric parameters and rotation speed. Since most extruder rates are measured in mass per unit time, the term Q_{md} is defined as the mass rotational flow:

$$Q_d = \frac{pV_{bz}WHF_d}{2} \tag{1.4}$$

$$Q_{md} = \frac{p\rho_m V_{bz}WHF_d}{2} \tag{1.5}$$

where ρ_m is the melt density at the average fluid temperature of the resin, V_{bz} is the z component of the screw velocity at the flight tip, W is the average width of the channel, p is the number of flight starts, H is the depth of the channel, and F_d is the shape factor for plane couette flow. The analysis using plane couette flow does not take into account the effect of the flights (channel helix) on the flow rate. For an infinitely wide channel, no flights, F_d would be equal to 1. As the channel width approaches the height, F_d is about 0.5. It is important to include the shape factors when evaluating commercial screw channels. This becomes extremely important for deep channels where H/W does not approach zero. An additional correction factor can be used to improve the calculation of the rotational flow term [1]. The shape factors are calculated as follows:

$$F_d = \frac{16W}{\pi^3 H}\sum_{i=1,3,5,\ldots}^{\infty}\frac{1}{i^3}\tanh\left(\frac{i\pi H}{2W}\right) \tag{1.6}$$

The velocity of the flight tip V_{bz} is calculated as follows:

$$V_{bz} = \pi N D_b \cos\theta_b \tag{1.7}$$

$$\tan\theta_b = \frac{L}{\pi D_b} \quad \text{thus} \quad \theta_b = \arctan\frac{L}{\pi D_b} \tag{1.8}$$

where N is the screw rotation rate in revolutions per second, D_b is the diameter of the inside barrel wall, L is the lead length, and θ_b is the helix angle at the barrel wall.

Because of the helical nature of the screw, the width of the channel is narrower at the core of the screw as compared to that at the barrel wall. The calculation of the rotational flow rate, however, requires the average width of the channel. The average width of the channel is calculated as follows:

$$W_b = \frac{L}{p}\cos\theta_b - e \tag{1.9}$$

$$W_c = \frac{L}{p}\cos\theta_c - e \tag{1.10}$$

$$\tan\theta_c = \frac{L}{\pi(D_b - 2H)} \quad \text{thus} \quad \theta_c = \arctan\frac{L}{\pi D_c} \tag{1.11}$$

$$W = \frac{W_b + W_c}{2} \tag{1.12}$$

where e is the width of the flight perpendicular to the edge, D_c is the diameter at the screw core, W_c is the channel width at the screw core, and θ_c is the helix angle at the screw core.

The volumetric pressure flow term, Q_p, and the mass flow pressure flow term, Q_{mp}, are computed as follows:

$$Q_p = \frac{pWH^3F_p}{12\eta}\left[\frac{\partial P}{\partial z}\right] \tag{1.13}$$

$$Q_{mp} = \frac{p\rho_m WH^3F_p}{12\eta}\left[\frac{\partial P}{\partial z}\right] \tag{1.14}$$

$$F_p = 1 - \frac{192H}{\pi^5 W}\sum_{i=1,3,5,\ldots}^{\infty}\frac{1}{i^5}\tanh\left(\frac{i\pi W}{2H}\right) \tag{1.15}$$

where F_p is the shape factor for pressure flow, $\partial P/\partial z$ is the pressure gradient in the channel in the z direction, and η is the shear viscosity of the molten polymer at the average channel temperature and at an average shear rate, $\dot{\gamma}$:

$$\dot{\gamma} = \frac{\pi D_c N}{H} \tag{1.16}$$

The shear rate in the channel contains contributions from the rotational motion of the screw and the pressure-driven flow. The calculation of the shear rate, $\dot{\gamma}$, using Eq. 1.16, is based on the rotational component only and ignores the smaller contribution due to pressure flow.

The relationship between the pressure gradient in the z direction to the axial direction, l, is as follows:

$$\frac{\partial P}{\partial z} = \frac{\partial P}{\partial l}\sin\theta_b \tag{1.17}$$

The pressure gradient is generally unknown, but the maximum that it can be for a single-stage extruder screw is simply the discharge pressure, P_{dis}, divided by the helical length of the metering section. This maximum gradient assumes that the pressure at the start of the metering section is zero. For a properly designed pro-

cess, the actual gradient will be less than this maximum, and the pressure at the start of the metering section will not be zero.

$$\frac{\partial P}{\partial z} = \frac{P_{dis} \sin \theta_b}{l_m} \tag{1.18}$$

where l_m is the axial length of the metering section.

The total mass flow rate, Q_m, is calculated by combining the flow components as provided in Eq. 1.19 for the total mass flow rate. An additional correction factor can be used to improve the calculation of the rotational flow term [1].

$$Q_m = \frac{p\rho_m V_{bz} WHF_d}{2} - \frac{p\rho_m WH^3 F_p}{12\eta}\left[\frac{\partial P}{\partial z}\right] \tag{1.19}$$

Estimation of the rate and pressure gradient using Eq. 1.19 should be performed for each troubleshooting operation. Examples for its use are available elsewhere [1].

For grooved-bore extruders, the design of the feed section including the grooves and screw section control the rate of the process. This calculation of the rate is considerably more complex and is out of the scope of this chapter. Grooved bore extruders are discussed in detail elsewhere [8–10].

1.3 Gels

A common contaminant in polyolefin film products is gels. The term gel is commonly used to refer to any small defect that distorts a film product, creating an optical distortion. There are many types of gels [11, 12], and the most common include (1) gels that are crosslinked via an oxidative process, (2) highly entangled resin gels (undispersed but not crosslinked), (3) unmelted resin, and (4) a different type of resin or contaminant such as wood, cloth fibers, or dirt. A crosslinked resin gel is typically formed during an oxidation process, resulting in the crosslinking of the resin chains and the generation of color bodies. These gels will not melt fully during analysis using a hot-stage microscope. Highly entangled gels are typically high molecular weight polymer chains that are highly entangled and thus difficult to disperse during the extrusion process. When analyzed using a hot-stage microscope, this gel type will melt as the stage temperature is increased. When the stage temperature is then decreased, the gel will crystallize before the surrounding material, creating the appearance of a gel. Since these gels are not oxidized they are not associated with color. They are commonly referred to as undispersed or unmixed gels. Unmelted resin exiting with the discharge can sometimes occur, especially at high extrusion rates. These gels will melt during heating with a hot-stage microscope,

and typically they will not re-form during the cooling phase. Numerous sophisticated methods are available for analyzing gels, including epi-fluorescence microscopy, polarized light microscopy, and electron microscopy with X-ray analysis.

Gels can be generated from many different sources and include (1) the resin manufacturer, (2) the converting process, (3) pellet blending of resins with significantly different shear viscosities, (4) pellet blending of different resin types, and (5) direct contamination. Modern resin manufacturing processes exclude oxygen from the system and are very streamlined such that process areas with long residence times do not exist. As such crosslinked and oxidative gels are likely not generated by the manufacturer. Improperly designed extrusion equipment and processes, however, are common, leading to the oxidative degradation of resins and crosslinked gels. Several case studies in the next sections show how poorly designed processing equipment can lead to crosslinked and unmixed gel contamination of products.

Established protocols for gel analysis in polymer films are well documented in the literature [11–14]. Typically a film with defects is visually inspected using a low power dissecting microscope. The gels can be classified based on size, color, and shape and isolated using a razor blade or scissors. Cross sections of the gels ranging from 5 μm to 10 μm thick are collected at temperatures below the glass transition (T_g) temperature of the film using a cryogenic microtome, about –80°C to –120°C. For optical examination, a thin section containing the gels is placed on a glass microscope slide with a drop of silicone oil and covered with a glass cover slip. Additional sections are collected for examination via hot-stage microscopy and for compositional identification if needed.

After collecting the sections, the remaining polished block-face containing the remainder of the gel is retained. In many instances, gels arise from inorganic contaminants such as the metals from pellet handling equipment, extruders, or components from masterbatches. Examination of these inorganic components are best performed with the block-face sample using a scanning electron microscope (SEM) equipped with an energy dispersive X-ray detector (EDX) [15, 16]. In some cases, additives or inorganic residues are present in low concentrations within the gels. A method to enrich the concentration of these materials is to expose the block-face containing the gel to oxygen plasma. Etching will preferentially remove the polymer at a much faster rate than the inorganic materials, enriching these components for elemental analyses. It must be noted that prior to SEM and EDX analyses, a thin conductive coating like carbon is typically evaporated onto the sample to render it conductive under the electron beam.

The most common type of gel is caused by oxidative processes that crosslink the PE chains. The best way to identify this gel type is by observation with polarized light and ultraviolet (UV) light sources. Transmitted polarized light microscopy represents an effective technique [17] that can be used to investigate structures in crys-

talline films. For example, black speck gels were contaminating a multilayer film product. The gels were relatively brittle when cut for analysis. The source was unknown. The detail of the gel is clearly visible using transmitted polarized light, as shown in Fig. 1.7(a). Close examination of this gel using epi-fluorescence with an ultraviolet light source caused an intense fluorescence emission, as shown in Fig. 1.7(b). This type of emission suggests thermal oxidation and crosslinking of the polymer. Microinfrared analysis of the gel indicated that it contained oxidized PE and maleic anhydride [1, 12]. This material likely formed on the metal surfaces of the extruder and then flaked off during a minor process instability. The material then flowed downstream and contaminated the film as a gel.

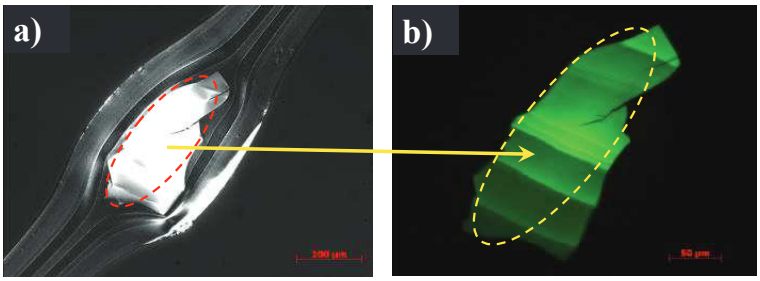

Figure 1.7 Transmitted polarized light images of a thermally oxidized and crosslinked gel in a multilayer film: (a) photograph in polarized light, and (b) the gel fluorescing under UV light [12]. Photographs were provided by E. Garcia-Meitin of The Dow Chemical Company

Crosslinked gels are oxidized gels, but the level of oxidation is not enough to cause them to fluoresce under UV light. The gels may have a level of crystallinity and thus be birefringent under polarized light. For example, the slightly birefringent gel shown in Fig. 1.8(a) was studied using a temperature-programmable, hot-stage, polarizing light microscope [16]. The optical melting temperature (T_m) of the gel was measured at 128°C and consistent with the PE used to make the product, as shown in Fig. 1.8(b). To determine if the gel was unmixed (highly entangled but not crosslinked), the gel was held above the melting temperature (135°C) and then stressed. A dental tool was used to stress the top of the glass slip cover. Crosslinked gels will appear birefringent, as shown in Fig. 1.8(c), in response to the anisotropy of stress distribution in the gel to polarized light. The gel dimensions and shape remained after cooling, verifying crosslinking, as shown in Fig. 1.8(d). If the gel was highly entangled and not crosslinked (unmixed gel), the gel would have disappeared after stress and cooling were applied.

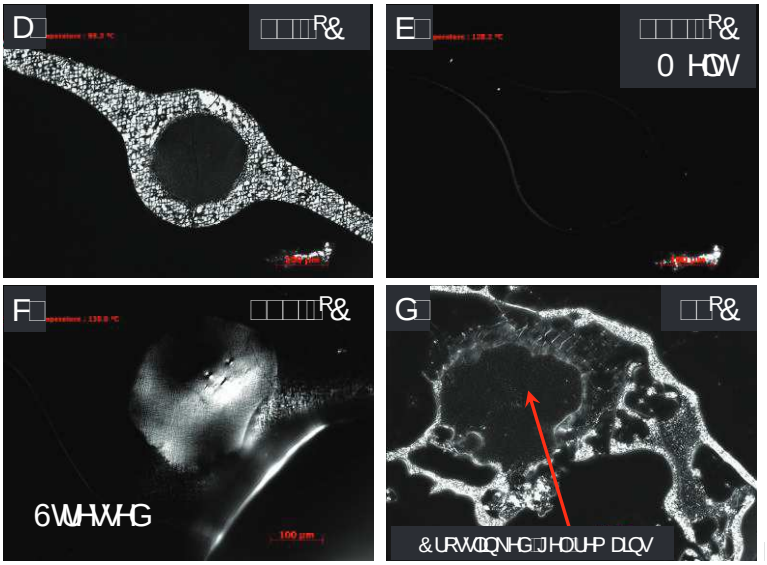

Figure 1.8 Hot-stage microscopy of a crosslinked gel in a crystalline monolayer film: (a) below the melting temperature, (b) optical melting point at 128°C, (c) appearance of birefringence after stressing at 135°C, and (d) intact crosslinked gel after cooling to 30°C [12]. Photographs were provided by E. Garcia-Meitin of The Dow Chemical Company

The origin of defects causing discoloration in polyolefin pellets can be identified using light and electron microscopy. For example, PE pellets from an in-plant recycle repelletizing process contained pellets that were off-color and had black specks, as shown in Fig. 1.9(a). One of these defects was isolated using the cross-sectioning technique, as shown in Fig. 1.9(b). The cross section revealed an intense reddish particle that caused the discoloration of the pellet. SEM and EDX microanalyses were used to determine that the defects contained primarily iron and oxygen, and it likely was iron oxide. A backscatter electron image (BEI) of the pellet block-face sample showed the defect causing the discoloration, and the elemental spectrum was shown to be iron oxide [1]. Metal-based defects can originate from process equipment, railcars used for shipment, pellet transfer lines, and poor housekeeping. The origin of the iron oxide was likely from a storage bin.

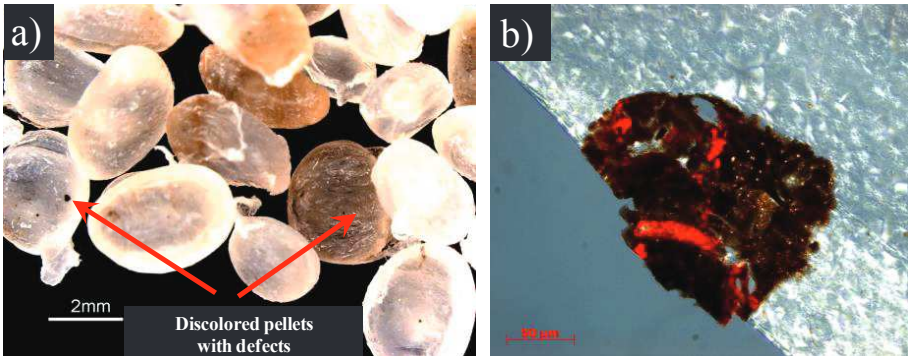

Figure 1.9 Photographs of foreign contamination in pellets of a repelletized reclaim stream: (a) photomicrograph of discolored PE pellets containing dark defects, and (b) transmitted polarized light micrograph of a pellet cross section containing a defect [12]. Photographs were provided by E. Garcia-Meitin of The Dow Chemical Company

In another example, a multilayer film product was experiencing occasional gels. The gels were isolated and the cross sections were collected as shown in Fig. 1.10(a). These gels contained highly birefringent particles that resided in the core layer. The outer film layers appeared amorphous, and the core layer was slightly birefringent. The optical melting temperature of the core layer was determined to be 123°C while the birefringent gels melted at 265°C. The melting temperature of 123°C was consistent with the polyethylene (PE) resin used to produce the core layer. The higher melting temperature of the material and microinfrared analyses of the defects indicate that they were foreign contaminants, and they were identified as a polyester resin. The polyester resin was used in another process in the converting plant, and it inadvertently contaminated the PE feedstock.

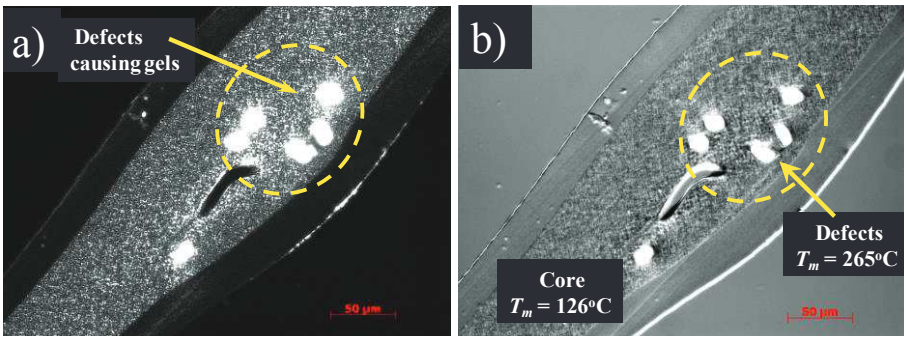

Figure 1.10 Photographs of gels in the core layer of a three-layer film: (a) transmitted polarized light, and (b) hot-stage microscopy was used to determine the melting temperatures of the core resin and defects [12]. Photographs were provided by E. Garcia-Meitin of The Dow Chemical Company

Another common contaminant that produces gels is fiber, as shown in Fig. 1.11. In many cases, these contaminants are cotton fibers from clothing and gloves or cellulosic fibers from packaging materials. Fourier transform infrared (FTIR) spectroscopy is one of the best techniques for determining the chemical functionality of organic-based defects in PE films.

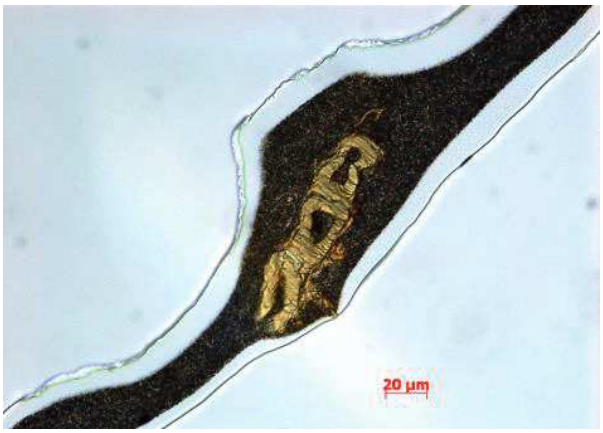

Figure 1.11 Transmitted bright-field image of a PE film containing a fibrous gel [12]

Once the contaminant is identified, the troubleshooter must determine how the material entered the feedstock stream. Process controls must be identified and implemented to mitigate the contaminant source.

1.4 Troubleshooting Extrusion Processes

Eventually every single-screw extrusion process will experience periods when the machine is operating at a performance level that is less than designed. During these periods, the cost of manufacturing will increase due to the production of off-specification products, loss of production rates, high levels of recycle, higher labor costs, and lower daily production of prime product. In extreme cases, the problem can be so severe that the line must be shut down. Obviously the plant needs to restore the operation of the line to the original performance level as soon as possible to maximize profitability. Many things can cause an extruder to malfunction, including mechanical and electrical failures, installation of new equipment, process changes, and resin changes. A complete process for troubleshooting an extrusion process can be obtained in reference 1. Several of the most common problems associated with film production processes are presented in this section.

1.4.1 Improper Shutdown of Processing Equipment

Shutting down an extrusion line occurs for many reasons, including planned shutdowns for maintenance, shift changes, changing filtering screens, product changes, and many unplanned events. A shutdown period is defined here as a period when the screw is not rotating and thus resin is not discharging from the line. If the shutdown period is relatively short such that very little resin degradation can occur, then the extruder barrel temperatures can be maintained at the operating set point temperatures. If the length of the shutdown is long relative to the time required to create a significant level of degradation products, then the extruder should be either purged with a more thermally stable resin or the barrel set point temperatures should be decreased to considerably lower temperatures. Purging the resin with an inert gas to exclude oxygen is also effective at mitigating gels [1]. An extruder that is maintained at process conditions long enough to create degradation products can be very difficult to bring back online running prime product. In this case, the surfaces of the screw and all metal surfaces in contact with molten resin may become coated with degradation products, as shown in Fig. 1.12. The time to purge them out can be extremely long and very expensive. For example, LLDPE resins can form crosslinked gels and black specks after 30 minutes of being off-line at process temperatures. If the shutdown is under 30 minutes, the barrel can be held at the process temperature. If the shutdown is longer but the line will be brought back online soon, the screw could be rotated at a low speed of 5 rpm to keep resin flowing, mitigating the formation of degradation products. For longer shutdown periods, the extruder should be purged using an LDPE resin and then cooled to ambient temperature.

Figure 1.12 Photograph of a screw that had numerous shutdowns where the extruder was maintained at operating temperatures for an extended time. The extruder was purged prior to removing the screw, yet dark degraded resin covers most areas of the screw [1]

Antioxidant chemicals are typically added at levels that stabilize the resin during normal melt processing. They are not meant to protect the resin from degradation during an extended shutdown period. Antioxidants are slowly consumed during the extrusion process, and thus they can be fully consumed during an extended shut-

down period. When they are fully consumed, the resin system is not protected from degradation, and thus degradation reactions will occur at accelerated rates.

1.4.2 Gel Showers in a Cast Film Process

Crosslinked gels can form in stagnant regions of screw channels, transfer lines, and dies. The time required for these gels to form range from about 30 minutes for linear low density polyethylene (LLDPE) resin up to 12 days for low density polyethylene (LDPE) resin. Stagnant regions can occur at entries and exits of mixers [1] and barrier sections, and they can occur when the metering channel of smooth-bore extruders is not controlling the rate. In these cases, a section upstream of the metering section is rate limiting, causing portions of the metering section to operate partially filled [18, 19]. When these channels operate partially filled, the main flow is on the pushing side of the channel while the trailing side operates void at first. After a period of time, clean resin gets into the void regions and rotates with the screw for long durations. Eventually the resin will degrade, forming crosslinked gels. Slight process upsets can dislodge this material, allowing the material to flow downstream, creating a gel shower in the film.

A film plant was extruding an LDPE resin into a specialty product using a cast film process [18, 19]. Due to high demand, a new 88.9 mm diameter, 33 L/D extruder was installed in the plant. Soon after start-up the product was acceptable and high quality. After 12 days, the line began to experience intermittent discharges of crosslinked material (gel showers) and carbon specks. Photographs of these gels are shown in Fig. 1.13. In some cases, the gel showers were observed two to three times per day and would last from 1 to 5 minutes. The gels were clearly crosslinked and were brown in color. The extrudate temperature was higher than expected for the process. The intermittent gels resulted in production downtime due to purging and in numerous customer complaints. A high and costly level of quality control was required to remove the gel-contaminated product from the prime product. Due to the high amount of downtime and the high levels of quality control needed, the operation of the new line was considerably more expensive than planned.

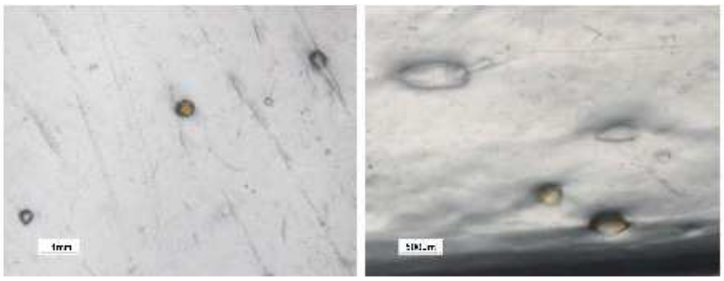

Figure 1.13 Photographs of crosslinked gels in an LDPE film

It was hypothesized that the extruder was operating partially full due to the low specific rate during operation. To determine if partially filled channels were the root cause of the reduced rate, high discharge temperature, and degraded material, screw rotation was stopped and the screw was removed while hot from the extruder. Examination of the polymer on the screw indicated that in the meter section about half of the channel width on the trailing sides of the flights for all but the last diameter were filled with a dark-colored, partially carbonized LDPE resin, indicating that these regions were stagnant. The reduced flow rate caused these regions to be partially filled, creating void regions on the trailing side of the channel. Some of the resin adhered to the trailing side of the screw in the void regions and stayed there for extended time periods, as shown in Figure 1.14. The resin adhering in the void regions eventually degraded into the dark-colored, crosslinked material. Small process variations dislodged some of this material and caused the intermittent gel showers that contaminated the product. Moreover, compacted solids were found wedged in the channel at the entrance to the barrier section. The wedged material was caused by the relatively large width of the entering solid bed being forced into the continually decreasing width of the solids channel of the barrier section.

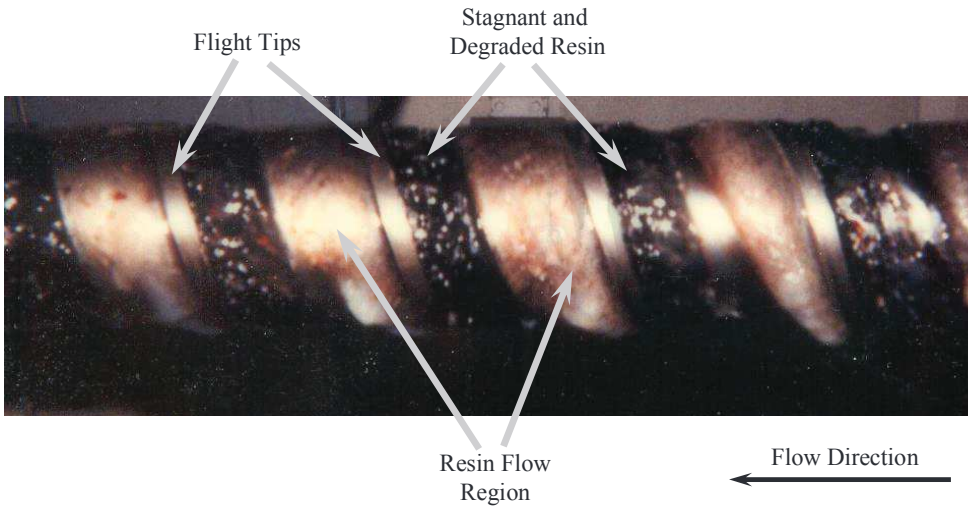

Figure 1.14 Photograph of a removed screw showing the resin flow and degraded resin due to stagnant regions [1]

The technical solution to eliminate this problem was a simple modification to the entry of the barrier melting section. For this modification [18], some of the metal in the melt conveying channel was removed along with a portion of the barrier flight, allowing some solid material to enter the melt channel and reducing the restriction at the entry. By reducing the restriction, the rate-limiting step of the process changed from the entry region of the barrier section to the metering section. After the modification was made, the gels were eliminated from the process.

Author Index

A

Adams 265
Agassant 102, 122, 134, 149, 165, 166, 167, 168, 169, 170, 171, 172, 175, 176, 177, 180, 181, 182, 184, 185, 186
Aird 134
Alamo 42
Alfrey Jr. 76, 85, 87, 120
Alothman 43
Amon 87, 88
André 122, 184
Anturkar 134, 172, 180
Arda 149
Armstrong 75
Asai 351
Asano 308
Ast 54
Athene 32
Avenas 165, 180
Avila-Orta 265

B

Babel 31, 33, 47, 62, 63
Baird 286
Balzano 351
Bar 13
Barone 350
Barq 134, 167, 168, 172
Beaulne 122, 129
Becker 79
Benkhoucha 102
Bertrand 126
Billon 134
Blackson 13, 14
Blid 286
Blyler 166
Bogue 121
Bosse 286
Bouamra 168
Bourgeois 129
Bourgin 167, 168, 172
Bourrigaud 168, 169, 180
Boyce 265
Braatz 184
Bradley 85, 87
Brancewitz 32, 34, 39, 42, 43
Bras 31, 45
Breil 211, 223
Briston 195
Brown 350
Buckley 53, 265
Bullwinkel 32, 34, 39, 42, 43, 44
Bunn 280
Burger 265
Butler 12, 13, 32, 113, 128, 129

C

Cain 122, 184
Cakmak 32, 265, 278, 316
Campbell 4, 9, 10, 12, 13, 14, 15, 16, 17, 18, 19, 20, 21, 22, 23, 31, 32, 33, 34, 39, 42, 43, 44, 47, 48, 50, 51, 52, 54, 55, 62, 63, 113, 114, 117, 120, 124, 232, 233, 235, 237, 250, 258, 259, 275, 278, 286, 290, 291, 316
Cao 33, 43, 44, 47, 48, 50, 51, 52, 54, 62, 63, 124
Carla 265
Carley 77, 78
Carneiro 113, 114, 117, 118
Carradini 350
Carreau 32, 42, 169, 170
Carrier 178
Castillo 113, 114, 117, 118
Chae 317
Chambon 181
Champchesnel 265
Chang 165, 166, 265
Chen 351
Cheng 350
Chisholm 76
Choi 31
Chu 42, 265
Chuang 317
Clark 267, 272, 279
Cleereman 76
Coates 87, 88, 92, 94, 96, 99
Coccorullo 350
Cogswell 350
Colombo 103
Combeaud 149

Cook 79
Corradini 350, 361
Cotto 134
Coyle 103, 117
Crochet 134
Cudby 350
Culberson 32, 39
Culter 73

D

Dabas 168, 169, 180
Darus 13, 14
David 286
Dealy 350
Debbaut 134
Dees 31
de Jeu 351
Demay 122, 134, 165, 166, 167, 169, 170, 171, 175, 176, 177, 178, 180, 181, 182, 184, 185, 186
Denn 122, 141, 144, 165, 166, 180, 182, 184, 350
DeRosa 350
De Witte 96, 97, 98, 99
d'Halewyn 134
Ding 32, 42
Dobroth 134
Doi 134, 136
Dooley 22, 23, 77, 79, 84
Doufas 122, 184
Drda 350
Drechsel 166
Du 351
Duffo 134
Dupret 42
Dupuy 168, 169, 180

E

Eichnorn 265
El Kissi 350
Elmoumni 351
Ente 166
Erwin 134
Ewing 126

F

Fahy 102
Fava 279
Finlayson 9
Fischer 182, 350, 351
Fisher 141, 144
Fortin 178
Fu 351
Funaki 134, 141, 142, 143, 351, 355, 360, 364, 366
Funatsu 134, 144, 146

G

Galante 42
Galay 32
Gammell 74
Gao 126
Garcia-Meitin 12, 13, 14, 15, 16, 17
Garner 280
Geil 350, 351
Gezovich 350
Ghaneh-Fard 32, 42, 169, 170
Ghanta 350
Ghiljels 166
Gieniewski 166
Giesekus 144
Gilbert 350
Gilmour 102
Gletin 350
Goldman 286
Gomez 350
Goodrum 79
Gough 87, 88
Govaert 351
Graves 32
Greco 317
Grubb 350
Guerra 13, 350
Gupta 117, 166

H

Han 31, 85, 87, 123, 184, 317, 351
Harashina 265
Hassan 265
Hatzikiriakos 165, 174, 350
Haudin 122, 134, 167, 168, 172, 184
Hayashi 286, 316, 317
Headley 85, 88
Hearle 265
Hemsley 13
Hendra 350
Henrichsen 122, 184
Hernandez 73
Hoffman 350
Horn 265
Hoshino 31, 32
Housiadas 126, 184
Housmans 351
Hristova 351
Hsiao 265, 350
Hsu 351
Hu 351
Huang 34, 48, 51, 62, 102
Hyun 19, 20, 21, 22, 23, 165, 166, 167, 171, 174, 181, 183, 184, 187

I

Ieki 265, 278
Ihim 265
Ikeda 281
Imai 350
Imamura 265, 278
Inn 350
Isaki 134, 136
Ishihara 141, 165, 182
Ito 134, 136, 272
Iwai 290
Iwamoto 316, 317, 350
Iyenger 134

J

Jabarin 194
Jaffe 265
Jarecki 183
Jenkins 84
Jo 317
Johnson 42
Jones 265
Jons 85, 88
Jung 165, 166, 167, 174, 181, 183, 184, 187

K

Kaji 350, 351
Kajiwara 134, 144, 146
Kamal 42, 122
Kamatani 288, 355
Kanai 33, 47, 54, 62, 63, 113, 114, 117, 120, 129, 134, 136, 137, 141, 142, 143, 145, 146, 147, 148, 149, 150, 151, 158, 169, 184, 232, 233, 235, 237, 238, 247, 249, 250, 256, 258, 260, 275, 278, 286, 287, 288, 290, 291, 292, 296, 302, 304, 305, 308, 311, 316, 317, 350, 351, 355, 360, 364, 366
Kanaya 350, 351
Kang 265, 316
Kanho 286
Karlbauer 7
Kase 134, 136, 141, 165, 182, 275, 316
Katan 195
Katoh 350
Katsumoto 144, 146
Kawai 272
Kawakami 265
Keller 31, 46
Kenner 265
Keskkula 317
Khan 265
Kikutani 265, 272
Kim 181, 183, 184, 265, 317
Kimura 308
Kitajima 147, 148, 149, 150, 350
Klein 7, 9
Knittel 128
Kodjie 12, 13, 14, 15, 16, 17
Koerber 220
Kohler 166, 183
Kohno 158
Kometani 145, 146, 147, 148, 149, 150, 350
Kondo 360
Konishi 350, 351
Kopytko 85, 86, 87, 88, 94, 96, 99, 100, 101
Kouba 102
Kral 102
Krexa 32, 34, 39, 42, 43
Kuramoto 256
Kuratani 355, 366
Kurtz 129, 130, 350
Kwack 31
Kyu 32, 38, 42

L

Laffargue 169, 170, 171, 184, 185, 186
Lafleur 32, 42, 126, 169, 170
Langowski 220
Lauritzen 350
Lavallee 96, 98
Lee 75, 166, 167, 181, 183, 184, 187
Lengalova 86, 87, 88
Lenz 32
Li 126, 351
Lindstrom 286
Liu 121, 351
Llana 265
Lorentz 265
Lund 220
Luo 122
Lusing 286

M

Maack 85, 87
Machin 31
Mack 286
Mackley 149, 350
Maddock 6, 22
Malincoico 317
Mandelkern 42
Mandell 350
Manley 265
Marchal 134
Marin 168, 169, 180
Martins 265
Martyn 87, 88, 92, 94, 96, 99
Matovich 182
Matsuba 350

Matsumoto 265, 278
Matsumura 145, 146, 147, 148, 149, 150, 350
Matsuo 182, 265
Matsuzawa 287, 288, 355
Mavridis 85, 87, 91, 102, 103
McHugh 122, 166, 183, 184
McMahon 48
Meijer 351
Men 351
Menges 54
Merten 149
Mezghani 350
Miayji 351
Michaeli 113
Migler 165, 174
Miki 232, 233, 235, 237, 316
Miller 350, 361
Minoshima 169
Mitsoulis 122, 129
Miyaji 351
Mizukami 350
Moffat 22
Monasse 122, 184
Monnerie 265
Moore 258
Mori 350
Morihara 286
Münstedt 149
Muslet 122

N

Na 351
Nagarajan 55, 58, 61, 62, 63
Nagasawa 31, 32
Nakamura 286
Nakao 272
Nash 286
Natta 350, 361
Naumovitz 84
Nishi 317
Nishida 350, 351
Nitta 351
Nobrega 113, 114, 117, 118
Nomura 350
Nonomura 250, 275, 316
Norton 46
Nye 31, 45

O

Obot 124
O'Brien 117
Oda 267, 272
Ogawa 351
Ogita 265
Ohlsson 181
Ohta 260
Okui 272
Oliver 76, 77, 78, 79
Ooki 265
Oura 317

P

Pantani 350
Parent 169, 170
Park 123, 184
Paul 317
Pearson 120, 129, 182, 184
Peiti 168
Perdikoulias 85, 87, 88, 102, 104, 105, 106, 113, 114, 117
Peters 126, 351
Petraccone 350
Petrie 54, 120, 129, 180, 184
Piau 350
Pirkle 184
Plucktaveesak 350
Polich 286
Polychronopoulos 113, 114, 117, 118
Potente 12
Predohl 54
Procter 102

R

Rahalkar 350
Raley 79
Ramamurthy 350
Ramanathan 85, 88
Ran 265
Rasmussen 32, 34, 39, 42, 43
Rastogi 351
Rauwendaal 102
Ree 32, 38, 42, 286
Rehg 85, 88
Reuschle 13
Rhee 316
Rhodes 32, 38
Robert 149
Robinson 286
Roozemond 351
Roth 167, 168, 172
Rowell 9
Ruese 350
Ruppel 126
Rutgers 350
Ryan 31, 32, 45

S

Saha 85, 86, 87, 88, 89, 90, 91, 92, 93, 94, 95, 96, 98, 99, 100, 101, 104, 105, 106, 117
Saillard 102
Saito 364
Sakai 146
Sakaki 134, 144
Sakamoto 250
Sakauchi 286, 287, 288, 291, 292, 296, 302, 304, 316, 355
Sarafrazi 122
Saul 118
Savargaonkar 13
Scheirs 13
Schoenberg 286
Schöppner 12
Schrauwen 351
Schrenk 76, 85, 87, 88, 103
Schuetz 286
Sebastian 102
Selke 73
Sergent 165
Sergot 265
Serhatkulu 32
Shah 182
Shanker 85, 88
Sharif 122
Shen 351
Shetty 85, 87
Shibayama 317, 350
Shimizu 272
Shin 166, 167, 181, 183, 184
Shroff 85, 87, 91
Sics 265
Sidriopoulos 54, 123, 124, 125, 126, 129
Silagy 134, 168, 169, 174, 175, 176, 177, 180, 181
Simon 118
Skaki 134
Slichter 350
Smith 134
Socrate 265
Sollogoub 134
Song 183, 184, 286, 316
Spalding 4, 9, 10, 12, 13, 14, 15, 16, 17, 18, 19, 20, 21, 22, 23
Spares 87, 88, 94
Spirgatis 126
Spoelstra 351
Spruiell 31, 32, 41, 42, 121, 279
Srinivas 350
Stanford 31, 45
Steenbakkers 351
Stein 32, 38, 42, 265, 272, 350
Stewart 350
Stolle 134
Suga 145, 146, 147, 148, 149, 150, 350
Sun 117
Supaphol 32, 41
Swartjes 351
Sweeney 33, 48, 50, 51, 52, 54
Swenson 79

T

Tabar 32, 38
Tadmor 7, 9
Takahashi 350
Takarada 272
Takashige 286, 290, 291, 305, 308, 311, 316, 317
Takayanagi 351
Takeda 317
Takenobu 31, 32
Takeo 134, 136
Takeuchi 232, 233, 235, 237, 316
Takino 260
Takubo 351
Tamura 256, 260
Tanaka 158, 350
Tanifuji 113, 114, 117, 118
Tanner 120, 122
Tant 32, 39
Tas 31
Tassin 265
Teutsch 83
Thiel 7
Thomas 286
Tian 123, 129
Titomanlio 350
Tobita 232, 233, 235, 237, 316
Tonelli 350
Toussaint 350
Toyoda 258, 316
Tsamopoulos 184
Tsou 350
Tsuboshima 286
Tsunashima 258, 316
Tzoganakis 85, 87, 88, 89, 90, 91, 93, 94, 95, 96, 99, 104, 105, 106, 117

U

Uehara 286, 287, 288, 291, 292, 296, 302, 304, 316, 355
Uenoyama 317
Unsal 265
Upmeier 80

V

van Aarsten 38
van Breemen 351

van der Beek 351
Veazy 128, 129
Vega 351
Vergnes 149, 165
Verhoyen 42
Vickers 31
Ville 350
Vincent 165
Viny 265
Vlachopoulos 54, 113, 114, 117, 118, 124, 125, 126
Vlcek 85, 86, 87, 88, 89, 90, 91, 93, 94, 95, 96, 99, 100, 101, 102, 113, 114, 117

W

Wagner 113, 223
Wakabayashi 158
Walter 286
Wang 317, 350, 351
White 31, 54, 57, 166, 169, 184, 267, 272, 286, 316
Wilkes 31
William 286
Willis 350
Winter 265, 351
Wyxkoff 350

X

Xiao 72, 74, 75, 77, 79, 84
Xu 122
Xue 87, 88

Y

Yagi 134, 136
Yamada 250, 260, 275, 286, 287, 288, 291, 292, 296, 302, 304, 305, 308, 316, 355, 364, 366
Yamaguchi 94
Yamamoto 94
Yamane 166
Yan 351
Yasumoto 94
Yeow 134, 172, 184
Yoon 350
Yoshida 238
Yoshii 258, 316
Yu 31
Yuon 184

Z

Zatloukal 85, 86, 87, 88, 89, 90, 91, 92, 93, 94, 95, 96, 97, 98, 99, 100, 101, 104, 105, 106, 117
Zhang 126, 351
Zhao 351
Zheng 351
Zhou 351
Ziabicki 183, 272
Zippenfeld 54
Zitzenbacher 7

Subject Index

Symbol

α crystal 261
β crystal 261

A

absolute black body radiation 53
additives 158
air knife 202
air rings 124
aluminum bubble 56
analyzer 43
annular die 30, 33
antioxidant chemicals 18
antistatic additive 158
apparent emissivity 53
apparent reflectivity 53
average intensity 40
Avrami kinetics 41, 42
axial position 40
axisymmetric instabilities 183

B

balance equation 288
barrier flighted screw 5
beta-gauge system 220
biaxially oriented film 232, 238
biaxially oriented tentering film 231, 234
biaxial stretching 194
birefringence 266, 271, 275
black body 52
– emissivity 53
– temperature 49
bleeding 158
– speed 159
blocking 156
blown film 73, 112, 119, 165
blow-up ratio (BUR) 112, 169, 184
BOPA 226
BOPE 227
BOPET 194, 226
BOPLA 227
BOPP 194, 196, 225, 238, 260
BOPS 227
boundary layer 58, 59, 61
bowing 250
– phenomena 250, 275
Bragg's law 279
branched polyethylene blends 42
bubble 112
– collapsing 127
– deformation 292
– forming 119
– instabilities 32
– velocity 34
bulk deformation 39
bulk temperature 51
BUR 112

C

capacitor 215, 226
carbon specks 22
Carreau-Yasuda equation 116
cast film 73, 164
CCD camera 43
chain-track system 205
chill roll 201
clips 205
CO_2 footprint 227
Coanda effect 124
coat hanger 78
COC 228
coefficient of static fiction 151
coextrusion 114, 198
– visualization 92
coherent light 32, 33
composition distribution 244
conservation law 52
contact winding 209
cooling 123
– air 34
– air flow 54
– phenomena 181
– process 239
– rate 45
– system 241
crater-like surface 260
critical Deborah number 181

critical draw ratio 167, 179
cross equation 116
crystalline morphology 31
crystallization 42, 47
– kinetics 32
cylinder plate 339

D

DDR 112
Deborah number 167, 180
deformation 34
– behavior 137
– histories 34
– rate 34
detect spherulites 360
die bolt adjustment 200
die design 117
die flow 111
– analysis 113
diffusion coefficients 158
direct drives 202
direct numerical simulation 173
dog bone defect 175
double bubble 195
double bubble tubular film 285–287, 291, 296, 301, 302, 304, 305, 307, 308, 311
– machine 287
– process 232, 319
down-gauging 228
drawdown ratio (DDR) 112
drawing instability 164
draw ratio 165, 169, 175, 184
draw resonance 141
– instability 165, 171

E

ease-of-tearing properties 333
easy-tear film 328
edge trim 209
edge views 279
eigenvalue 173, 179, 184
electrostatic 203
– pinning 236
Elmendorf tearing test (ASTM D1922) machine 333
elongation viscosity 180
emissivity 48–50
end view 280
entangled gels 12
equi-biaxial stretching 270
equipment producers 72
EVOH 286
Ewald sphere 278
extrusion 198

F

fiber spinning 164, 182
filament breakage 167
film 50
– blowing 111, 169, 183
– breakage 143
– casting 134, 135, 136, 146
– cooling 46
– drawing machine 265
– extrusion 70
– properties 62, 295
– structures 72
– tentering machine 275
– thickness 47, 48, 50
– velocity 43
filtration 199
flat-panel displays 226
flat-screen displays 216
flight radii 22
flow analysis 102
flux measurements 61
four-lobed pattern 37
freeze-frost line 29
freeze line 31, 47
freeze line height (FLH) 123
frozen-in strain 50

G

Gammell 75
gels 12
gel showers 19
generalized Newtonian fluid model (GNF) 115
Giesekus model 144
GNF 115
growth 41

H

haze 151, 157
HDPE 157
heat flux 56, 57
– meters 55
heat loss 47
heat recovery systems 207
heat seal temperature 151, 155, 156
heat setting 280
– zones 275
heat transfer 30, 201
– coefficient (U) 36, 46, 53, 54, 60, 137
He-Ne laser 43
Henky strains 35
higher-order structure 264

I

IBC 113, 126
impact strength 153, 320, 332
impingement 46
improper shutdown of processing equipment 18
infrared detector 51
infrared (IR) absorption 220
infrared temperature 30
in-line coater 223
inorganic contaminants 13
in situ observation 253, 254
instability 141, 241
integrated process control (IPC) 217
interfacial instabilities 85
interfacial shear stress 87
internal bubble cooling (IBC) 31, 113, 126
interplanar spacing 279
intrinsic birefringence 281
IR surface temperature 33
isotropic 215

K

Kuhn statistical theory 273

L

laboratory extruder 223
laboratory tenter stretched film 296
lab stretcher 223
lamellae 31
laminar flow 57
LCD 228
LDPE 146
light scattered 32
linear motor 212
linear stability analysis 173, 182
LISIM 252
– technology 211
Lithium-ion batteries 228
LLDPE 152, 153, 156, 157, 302
local temperature 50
longitudinal stretching 241
Lorentz-Lorenz equation 281

M

Maddock-style mixers 6
mass flow 34
– rate 35
material design 301
MD and TD properties 62
MDO 203
melt fracture 147, 150
Melt Index (MI) 301
melt pumps 199
melt temperature 45
membrane approximation 183
membrane model 175
membranes 228
microscopy 32
Moffat eddies 22
molecular orientation angle (MOA) 220
monoaxial stretching 195
motorized table 33
multigap stretching 204
multilayer 198, 224
multimanifold die 77
MXD6 307, 308, 329, 340

N

neck-in 175, 181
necking 144, 146, 243, 244
nip speed 34
nonaxisymmetric instability 169, 183
noncontact system 48
noncontact temperature 33
normalized plastic strain 63
nozzle boxes 207
nucleation 41

O

off-center positions 275
OLED 228
online SALS 32
OPET 237
OPP 236
OPS 237, 291
optical 215
– anisotropy 265, 276
– axis 275
– film 226
– retardation 265
organic electronics 216, 226
orientation 31
oscillations 32
oxidative gels 13

P

PA 232
PA6 286, 305, 308, 329, 339
partially oriented yarn 272
PC 228
PE 286
periodic fluctuations 167
periodic instabilities 166
periodic oscillations 41
PET 236, 258, 259, 286

phase change 54
phase shift 266
physical crosslinks 31, 63
physical properties 151, 152, 157, 257
pilot line 222
pinning 202
planar elongation 269
planar orientation 274, 281
plastic strain 31
PMMA 228
polarizability 281
polarized fluorescence technique 327
polarized light 32
polyamide 232
polyethylene (PE) 136, 302
polyethylene terephthalate (PET) 232, 264
polymer chains 31
polymer processing aids 96
polypropylene (PP) 136, 146, 159, 232, 238, 304
polystyrene 232
power law equation 116
POY 272
PP 154, 159, 238, 244, 259, 260, 286
PPS 286
predicted temperature 36
preferential orientation 281
preheating 203
– process 287
– zone 275
pressure flow 11
pull roll stand 208
puncture resistance 226
PVDC 286

Q

quality data management system (QDM) 221
quick quenching 358
quiescent cooling 39

R

radial fibrils 31
radiation 47
– spectrum 48
radius 34
raman spectroscopy 32
reciprocal lattice vector 279
reciprocal space 279
reflectivity 49
refraction 32
refractive index ellipsoid 274
refractive indices 268
relaxation 214, 267
– time 63, 246
representative SALS images 37
resin degradation 18
rheological models 62
roll data history module (RDH) 221
roller chains 205
RTD 48
rubber elasticity theory 273

S

SALS 30, 32
– equipment 33
– images 40
– patterns 37
saturation solubility 159
SAXS 32
scale-up rule 308
scattering intensity 43, 45
screen 43
screw rotational flow 9
secondary crystallization 42
second invariant 115
second (scalar) invariant 115
self-ordering 282
semicrystalline polymer 31, 47
separator film 228
sequential biaxial stretching 233, 273, 311, 319
sequential stretching 232
shark skin 147, 149
shrinkability 299
shrinkage 214, 296
– stress 291
sigmoidal curve 41
simultaneous biaxial stretching 311, 319
simultaneous stretching 211, 232
single-flighted screw 4
single manifold die 76
single-screw extruders 2
sliding chain track systems 206
slip agents 158
slippage 156
small-angle light scattering device (SALS) 30, 338
solar back sheets 226
solubility 158
spatial intensity 38
spherulites 42, 44
spherulitic 31
spherulitic crystalline structure 30
spider die 79
spiral 113
– die 114, 117
spiral mandrel die 80
spontaneous structural ordering 272
stability curve 186
stackable die 84
Stanton number 174, 182

steady state 34
straight line cut 334, 335
strain 34
strain energy potential function 273
strain-hardening 268
strain rate 34, 35, 63
stress 50, 271
stress-optical coefficient 272
stress-optical rule 268, 272
stress-strain curve 323
stress-strain pattern 324
stress-strain relationship 214
stress versus birefringence behavior 272
stretching force 168
stretching patterns 214
stretching process 241, 287
stretching stress 329
stretching temperature 203
structure development 253
structure-processing property 69
substitution 228
superstructure 152
surface roughness 147, 149, 260
surface temperature 43, 51
surface tracking method 177

T

TAC 228
tacticity 244
take-up ratio (TUR) 112
tandem extruder 234
T-die casting 135–137, 143, 152, 242
TDO 205
tearing resistance 333
technology center 222
TEM 338
temperature 43, 47, 48, 50, 52
– plateau 36, 37, 47
TEM photographs 337
tension control 209
tentering process 232, 319
tentering zone 275
theoretical analysis 135, 287
theoretical equations 141
thermal isolation 83
thermal-transfer film 226
thermistor 48
thermocouple 48
thermosetting 205
thickness 43
– control 218
– uniformity 305, 340
thinning 61
thin polymer films 29
thin shell approximation 121
three-dimensional analyses 268
through view 279
tilting 275
time elapsed 36
time to crystallization 34
TNSD sign stability criterion 87
transient heat transfer 56
transmission electron microscope (TEM) 336, 366
transmissivity 49
transparency 157, 365
TREF (temperature rising elution fractionation) 155, 156, 301, 302
troubleshooting extrusion processes 17
true stress 267
tubular blown film 29
tubular film 113, 119, 135, 308
tubular process 319
TUR 112
turbulence 54
twin-screw extruder 199, 234
two-dimensional heat transfer model 54
two-stage mechanism 44

U

UDY 272
unattainable drawing region 180
unattainable region 182
unattainable zone 169
undrawn yarn 272
uniaxial stretching 267, 268
unit cell 280
unmixed gels 21
uptime 218
UV stabilizers 158

V

velocity 34
– measurements 61
Venturi effect 124
viscoelastic behavior 180
viscoelasticity 122
viscoelastic model 144
viscoelastic-plastic 62
visco-plastic 62
visualization 253
volume-filling spherulites 39

W

wave type of interfacial instabilities 87
WAXD 278
WAXS 32
web inspection 221

weight percent HDPE 43
Weissenberg number 122
wide-angle X-ray diffraction (WAXD) 278
– patterns 326
winder 209
worn screw 23

X

X-ray radiation 220

Z

zigzag interfacial instabilities 96